Fundamentals of Animal Cell Encapsulation and Immobilization

Mattheus F. A. Goosen, Ph.D.
Department of Chemical Engineering
Queen's University
Kingston, Ontario

CRC Press
Boca Raton Ann Arbor London Tokyo

Chapter 6

SCALE-UP OF GEL BEAD AND MICROCAPSULE PRODUCTION IN CELL IMMOBILIZATION

Denis Poncelet, Brigitte Poncelet De Smet, Chantal Beaulieu, and Ronald J. Neufeld

TABLE OF CONTENTS

5944-9/93/$0.00+$.50

I. INTRODUCTION

Immobilization systems compatible with many biocatalysts have involved the use of various gel-forming proteins (gelatin), polysaccharides (agar, calcium alginate, and κ-carrageenan), and synthetic polymers (polyacrylamide). Early techniques involved the formation of gel matrices in molds, entrapping biological cells. The gels could be manually portioned into small pieces of typically 2 to 5 mm.[1-4] Smaller spherical carriers were later formulated by dispensing droplets of the pregel suspension containing the immobilizant into a hardening solution.[2,5] A finer dispersion was achieved by emulsifying the gel in an oil phase and hardening the drops by internal gelation.[6-9] A membrane may be formed on the bead surface by immersing the beads in a suitable polymer-coating solution,[10,11] and if desired, the internal gel structure is solubilized and the gel material extracted, resulting in a membrane-bound microcapsule.[10] Direct microencapsulation involves dispensing droplets of an ionically charged gel solution into a polymer solution with opposite charge.[12-14] Presently, research is directed toward direct encapsulation of cells via interfacial polymerization around dispersed droplets of a cell suspension emulsified within a nonaqueous hydrophobic fluid.[15]

Most procedures giving rise to gel beads or microcapsules begin by dispersing the immobilizant in aqueous suspension, within the gel-hardening or membrane-forming solution. Following gelation or membrane formation, the entrapped cells are separated and washed. Industrial production not only implies scale-up, but also the need to reproducibly control the carrier properties. The size distribution of the droplets in the initial dispersion has a direct impact on the subsequent entrapment procedures and carrier properties. For example, the process of gelification and/or membrane formation is influenced by the droplet diameter.[16] Moreover, mass transfer is directly proportional to the surface area of the spherical beads, and resistance to shear breakage in a shear environment is related to the fourth power of the particle diameter.[17] In a continuous flow bioreactor, small beads or microcapsules may be lost in the outflow, while large carriers require a minimal level of agitation to be maintained in suspension. For some medical applications, microcapsules may be injected through a syringe needle, while very small microcarriers may be adsorbed by the tissues.

One of the objectives in cell encapsulation is to provide protection from shear forces prevailing in the bioreactor or during handling procedures. However, bead or microcapsule formulation itself involves dispersive forces. Equipment for the generation of liquid droplets must then be designed to minimize the shear applied to the cells, while achieving a homogeneous distribution of cells within the carriers.

The encapsulation of reagents such as drugs and pesticides is presently conducted on a large scale, often involving batches of several cubic meters.

However, the processing operations involving atomization, batch emulsification, and centrifugal techniques are often not suitable for live-cell encapsulation, due to shear effects. In contrast, most published studies involving cell encapsulation have been restricted to a small scale, often to a few milliliters.

Techniques which will permit control of scale-up operations and ensure control over size, shear, and cell distribution in the entrapment of live cells are described in this chapter.

II. DISPERSION METHODS

Two methods of dispersion are usually applied in cell immobilization: extrusion and emulsification. In the extrusion technique, often referred to as the the drop method, solutions are extruded through a small tube or needle, permitting the formed droplets to freely fall into a hardening solution. The droplets may also be cross-linked by addition of an appropriate reagent to the receiving solution. A typical example is the formation of alginate beads by dropping a sodium alginate solution into that containing calcium chloride.

In the emulsification technique, solutions are mixed and dispersed in a nonmiscible phase often facilitated with a surfactant. When the dispersion equilibrium is reached, hardening and/or membrane formation is initiated by cooling and/or addition of a gelling agent to the emulsion, or by introduction of a cross-linking agent. Thus, agarose beads are formed by emulsification in oil at about 45°C and the gel is set by a drop in temperature.[18,19] Nylon membrane-bound microcapsules are produced by emulsification of a diamine solution in an organic solvent, followed by addition of a dichloride, which reacts with the diamine at the droplet interface.[20]

A. EXTRUSION UNDER GRAVITY FORCE

The simplest method for dispensing individual liquid droplets is to permit the liquid to fall from the tip of a tube under the force of gravity. The mass of the droplet, m, may be computed by equalizing the gravity force, $m \cdot g$, with the product of the interfacial tension, g, and the perimeter of the tip, $2\pi d_e$ (Tate's law):

$$m\, g = \pi\, d_e\, \gamma \qquad (1)$$

where g is the gravity constant, d_e is the external tip diameter, and γ is the liquid surface tension. Equation 1 does not accurately determine the droplet weight because it does not account for the fact that the weight is also a function of the shape at the moment the droplet is released from the tip.[21] When instability of the droplet begins, the drop first stretches out, then breakage occurs under the needle tip, leaving a portion of the pendant drop

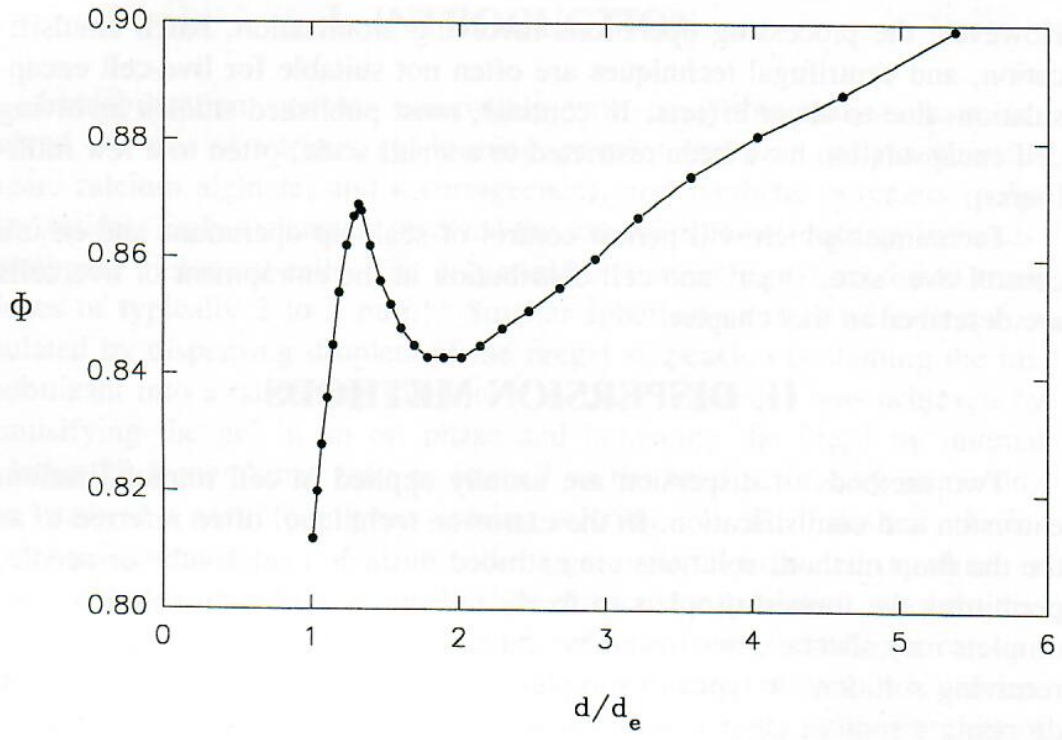

FIGURE 1. Real-to-ideal droplets ratio. (Computed from data of Reference 21).

behind. Equation 1 may be corrected according to Harkins and Brown[21] (Figure 1):

$$m\ g = \pi\ d_e\ \gamma\ \Phi^3 \tag{2}$$

where Φ represents the ratio between the real and ideal droplet diameters and is a complex nonlinear function of the tip and droplet diameters, d_e and d.[21] The mass of the droplet may be also estimated by:

$$m = \frac{\pi}{6} d^3\ \rho_d \tag{3}$$

where ρ_d is the density of the dispersed phase. Combining Equations 2 and 3 leads to:

$$d = \left(\frac{6 d_e \gamma \Phi^3}{g\ \rho_d}\right)^{1/3} \tag{4}$$

Figure 2 illustrates the droplet size computed as a function of the needle diameter. It is clear that the diameter of droplets obtained by extrusion under gravity is still larger than 1 mm, even with very small needle diameters. The bead or microcapsule diameter may differ from the expected value due to

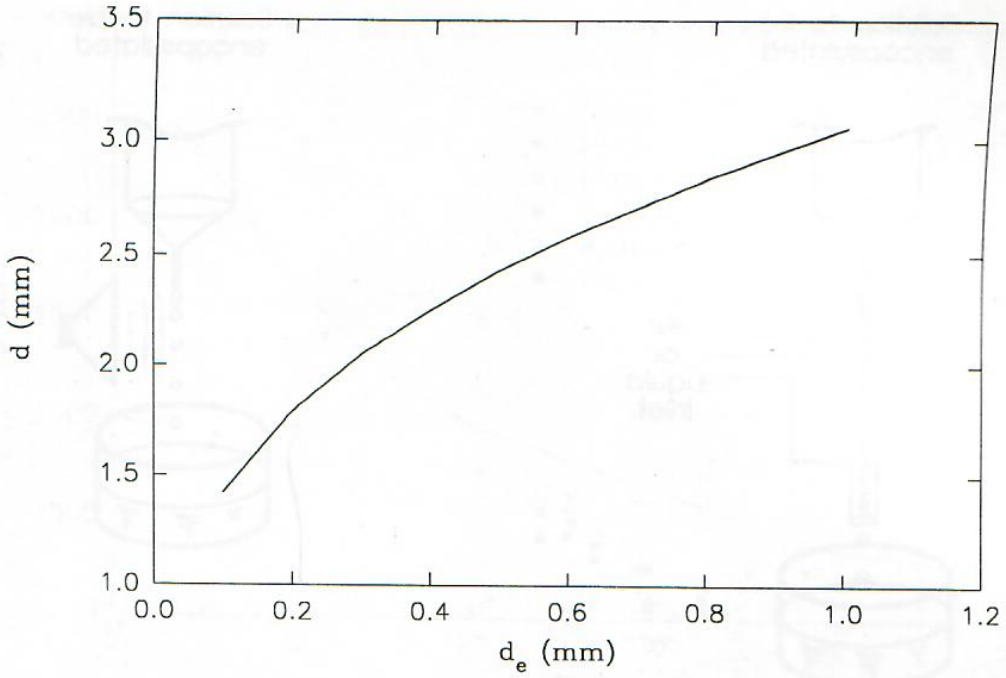

FIGURE 2. Diameter for droplets formed by extrusion under gravity.

swelling or shrinkage during the entrapment or encapsulation procedures. This has been observed with all dispersion methods. For example, alginate bead volumes are reduced by half during hardening, resulting in beads of about 2 mm formed from commercial tips.[1,14] In contrast, nylon microcapsules swell by a factor of 1.3 during washing.[22] Nylon microcapsules, generated with aqueous diamine droplets falling into di- or triacid chloride solutions, exhibit diameters between 2 and 2.5 mm.[23]

Smaller uniform-diameter beads are often desirable for some applications such as syringe injection. Other advantages include reduced mass transfer limitations and an increase in mechanical strength. Several techniques for reducing bead diameters have been developed and are illustrated in Figure 3. The procedures include air or liquid jets impinging on a needle,[24,25] electrostatic systems,[26] vibrating needles,[27] and emulsification techniques.[28,29]

B. EXTRUSION UNDER COAXIAL LIQUID OR AIR JET

Lane[30] proposed, in 1947, the application of an air jet around a needle to increase the force available to break a nascent drop from a suspending tip (Figure 3). In 1977, Charwat[25] replaced the air by a liquid jet, permitting the control of viscosity, surface tension, and the density of the continuous or entraining phase through selection of an appropriate liquid.

Assuming that the droplet has a larger diameter than the extrusion needle, the droplet diameter may be obtained by equalizing the sum of the drag and gravity forces with the surface tension force:

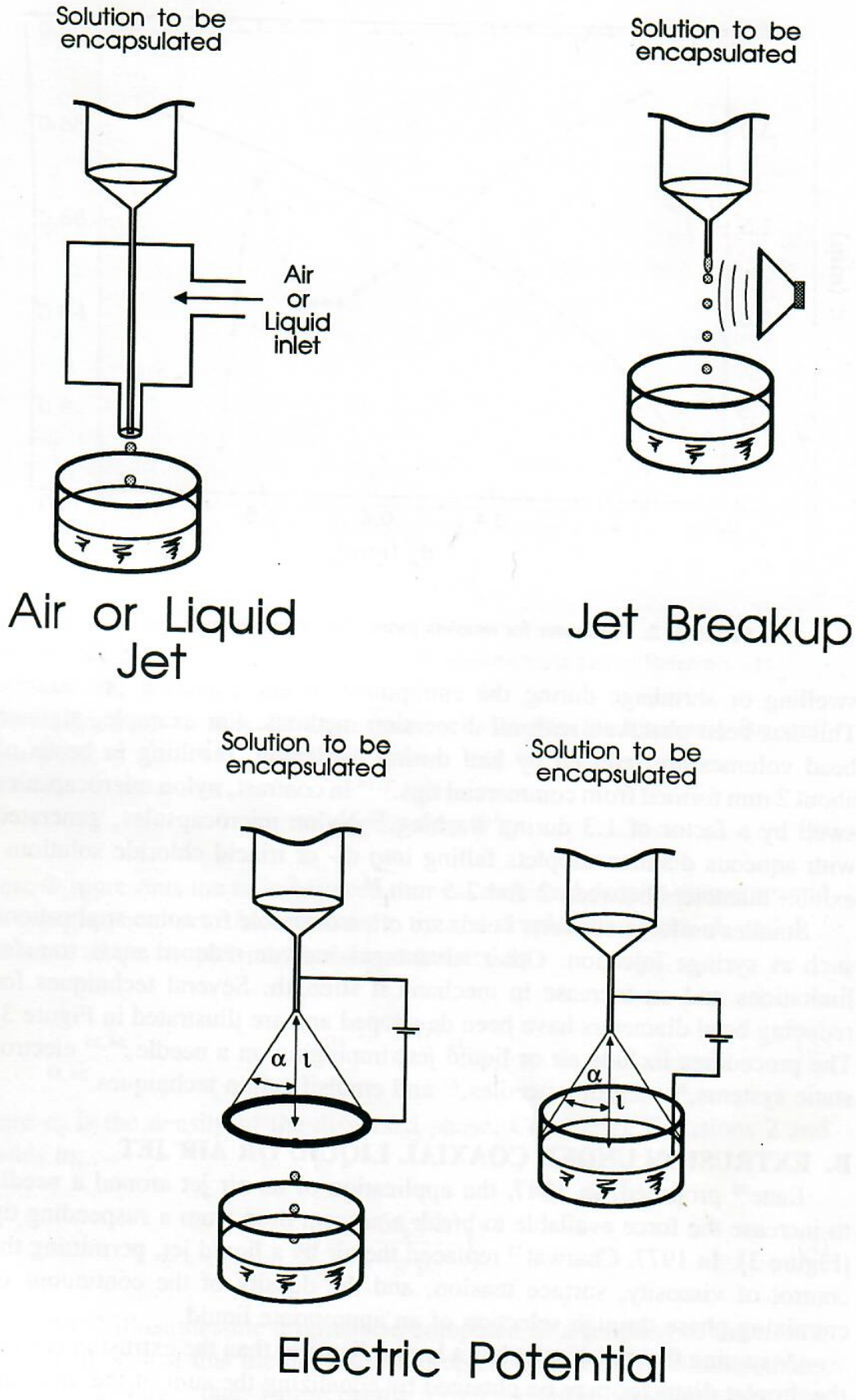

FIGURE 3. Droplet formation or extrusion methods.

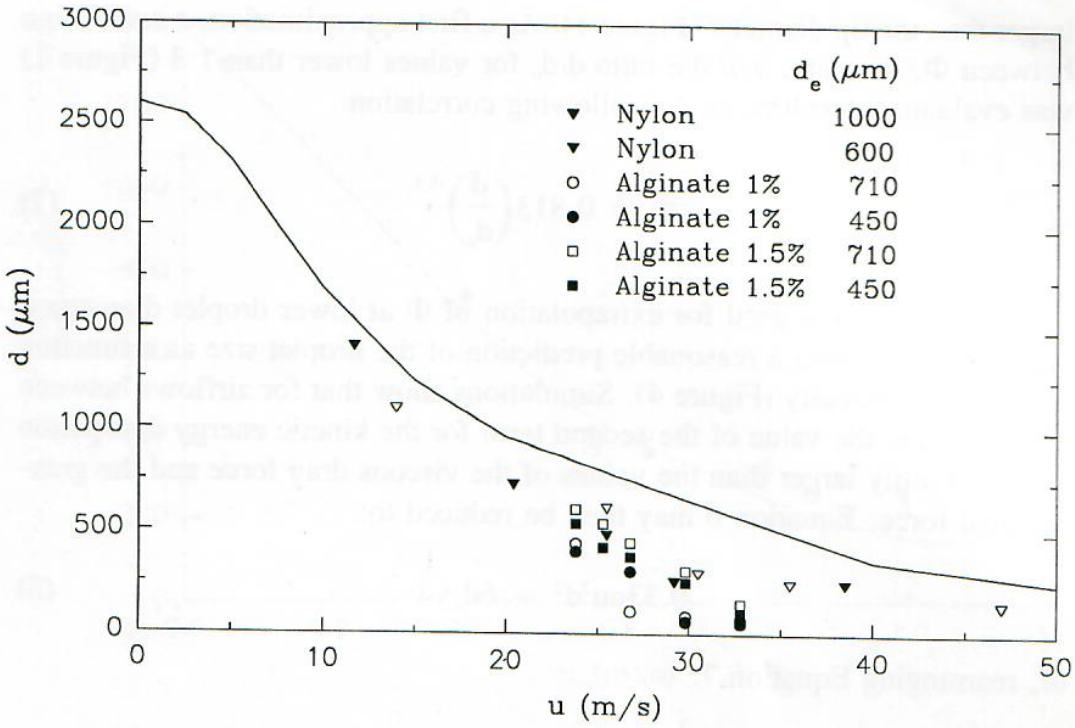

FIGURE 4. Control of the drop diameter with a coaxial air jet. (From data of References 33 and 34; data for simulation from Table 1.)

$$3\pi\mu ud + 0.055\pi\rho u^2d^2 + \frac{\pi}{6}d^3(\rho_d - \rho) = \pi d_e\gamma\Phi^3 \qquad (5)$$

The first term represents the viscous drag force, with μ the continuous phase (jet) viscosity and u the jet velocity.[31] The second term corresponds to the kinetic energy dissipation term,[32] with ρ the continuous phase density. Correction for the droplet density has been introduced in the gravity force term to take into account the buoyancy force when a liquid jet is used. After simplification, Equation 5 becomes:

$$18\mu ud + 0.33\rho u^2d^2 + d^3(\rho_d - \rho) = 6d_e\gamma\Phi^3 \qquad (6)$$

Equation 6 is only valid for beads larger than the tip diameter. The objective is to produce smaller beads. The nascent drop may then not be spherical, and the presence of the needle will perturb the drag force. Second, the diameter of the droplet-contacting surface is less than the needle diameter, and the needle diameter will have less of an impact on the droplet size. Moreover, at the needle tip, the airflow will create a depression, pinching and breaking the droplet.

Equation 6 was used to compute diameters, which were compared to data obtained from air jet-produced nylon microcapsules[33] and that of alginate beads (Figure 4).[34] Φ-Values are only presented for bead sizes equal to or

larger than the tip diameter (Figure 1). As a first approximation, a correlation between Φ, the data, and the ratio d/d_e for values lower than 1.3 (Figure 1) was evaluated, resulting in the following correlation:

$$\Phi = 0.813\left(\frac{d}{d_e}\right)^{0.3} \tag{7}$$

Equation 7 was used for extrapolation of Φ at lower droplet diameters. Equation 6 provides a reasonable prediction of the droplet size as a function of the air jet velocity (Figure 4). Simulations show that for airflows between 10 to 50 m/s, the value of the second term for the kinetic energy dissipation is significantly larger than the values of the viscous drag force and the gravitational force. Equation 6 may then be reduced to:

$$0.33\rho u^2 d^2 = 6 d_e \gamma \Phi^3 \tag{8}$$

or, rearranging Equation 7:

$$\frac{d}{\Phi^{1.5}} = \left(\frac{18 d_e \gamma}{\rho}\right)^{1/2} u^{-1} \tag{9}$$

Equation 9 slightly overestimates the droplet diameter, but agrees with a correlation proposed by Nukiyama and Tanazawa[35] for the atomization of volatile oil by use of a liquid-air nozzle. Nylon microcapsule diameters appear to be related to the air velocity at 1.65 power.[33] Additional data are required to clearly understand the relationship between d and Φ for small droplet diameters.

The range of air jet velocity applied in the production of alginate beads[34] is too limited to perform an accurate fitting. However, the data indicate that the droplet solution viscosity influences the value of Φ, which is proportional to the 0.4 power of the viscosity. Liquid flows up to 90 $cm^3\ h^{-1}$ have little influence on bead size. For higher flows, a broad size distribution was obtained.[34]

Combining Equations 7 and 9 indicates that the needle diameter has a minimal influence on the droplet diameter. In fact, the diameter of alginate beads[34] or nylon microcapsules[33] is also only slightly dependent on the needle diameter.

With a liquid coaxial flow, the correlation between Equation 6 and data obtained from the literature is improved over that observed with air jets (Figure 5). Simulations indicate that both the viscous drag force (10%) and the energy dissipation terms (90%) influence droplet size. The diameter is inversely proportional to the flow velocity (Figure 5), and it appears that Φ is relatively independent of droplet size. Lack of data limits further definition of a relationship between Φ and the working parameters.

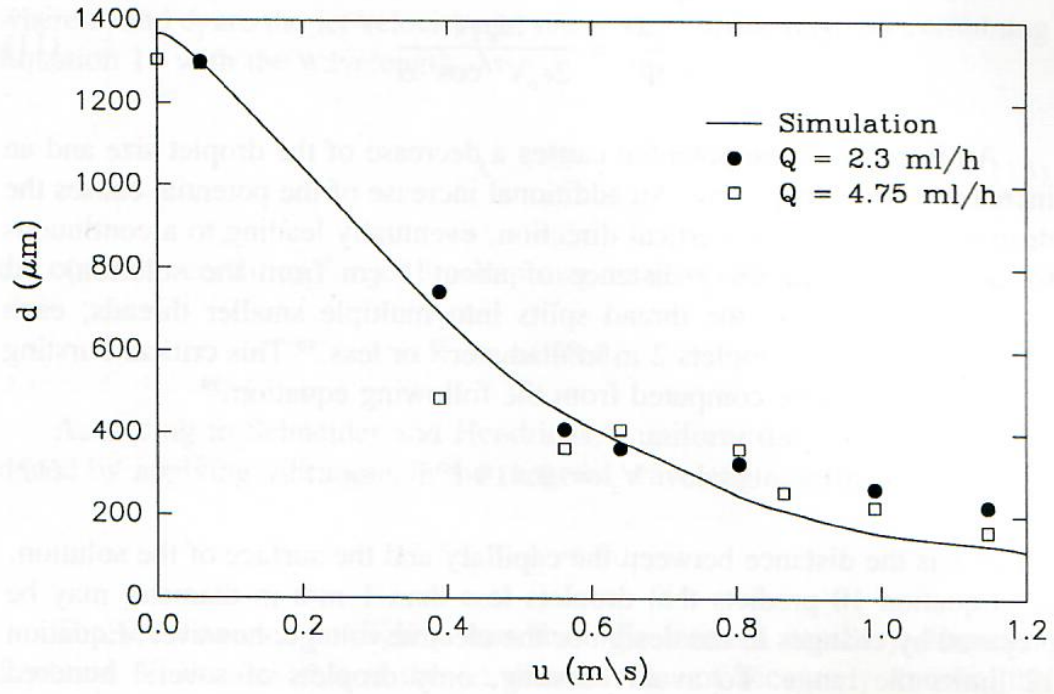

FIGURE 5. Droplet diameter vs. coaxial liquid jet velocity. (Computed from data of Reference 25; data for simulation from Table 1.)

Studies on cell encapsulation have been largely based on air-jet systems; however, liquid jets have received limited interest.[36-38] Both systems permit the preparation of microcapsules or beads with diameters ranging from a few microns to 1 ml. Lower jet velocities for liquid systems may offer the advantage of reduced shear and turbulence.

C. DROP FORMATION UNDER ELECTROSTATIC POTENTIAL

Drop formation is greatly improved by replacing the drag force required to detach droplets from the dispensing capillary tube with a high static potential between the capillary and the collecting solution (Figure 3).[39] Alternatively, the electric potential may be applied between the capillary and a stainless steel ring placed under the capillary (Figure 3).[26] The electric force, F, applied on the drop is equal to:

$$F = \frac{2\pi\epsilon_o dV^2}{\ell} \cos^a \alpha \qquad (10)$$

where ϵ_o is the electric permittivity constant (8.85×10^{-12}), V is the static voltage, and ℓ is the distance between the capillary and the surface of opposite charge α is defined in Figure 3 and factor a is equal to 1 for connection to the collecting vessel and equal to 2 for connection to a ring. Neglecting gravitational forces, the balance between the electric force and the surface tension forces, and isolating the drop diameter, leads to:

$$\frac{d}{\Phi^3} = \frac{d_e \gamma \ell}{2\epsilon_o V^2 \cos^a \alpha} \quad (11)$$

An increase of the potential causes a decrease of the droplet size and an increase in drop frequency. An additional increase of the potential causes the drop to elongate in the vertical direction, eventually leading to a continuous thread (2.5 kV, capillary distance of about 1 cm from the solution). At approximately 3 kV, the thread splits into multiple smaller threads, each consisting of small droplets 2 m in diameter[39] or less.[40] This critical bursting voltage, V_c, may be computed from the following equation:[39]

$$V_c = 9.419\ \ell^{0.2} \quad (12)$$

where ℓ is the distance between the capillary and the surface of the solution.

Equation 10 predicts that droplets less than 1 mm in diameter may be prepared by changes in the design or the electric voltage, however, Equation 12 limits the range. To avoid bursting, only droplets of several hundred micrometers may be prepared. Hommel et al.[26] proposed a related method to prepare beads in the range of 100 to 200 μm. The continuous static voltage was replaced by very short pulses (1 to 6 ms) with a controlled frequency (10 to 100 s^{-1}). The size of the droplet is then given by:

$$\frac{\pi}{6} d^3 = \frac{Q}{f} \quad (13)$$

where Q is the liquid flow rate and f the pulse frequency. This equation implies that the electric force is sufficiently large to separate the drop from the capillary, but not large enough to avoid bursting. When very short pulses are applied, the electric potential may even surpass the critical bursting potential.

The use of electrical potential for the production of beads has been patented;[26] however, no data exist in the literature to test the fit of the above equations.

D. BREAKUP OF CAPILLARY JET

If the liquid in the capillary tube exceeds a certain velocity, it exits from the tube as a jet. Capillary jets are unstable and break easily, forming small droplets.[41] Rayleigh[42] vibrated the jet with sonic waves (Figure 3), which at an optimum frequency, f, led to a stream of uniform droplets:

$$f = \frac{u_j}{4.058 d_j} \quad (14)$$

where u_j and d_j are the jet velocity and diameter, respectively. By combining Equation 14 with the wavelength, λ

$$\lambda = \frac{u_j}{f} \tag{15}$$

the optimum condition for jet breakup may be rewritten as:

$$\lambda = 4.058\ d_j \tag{16}$$

According to Schneider and Hendricks,[43] uniform droplets may be produced by applying vibrations in the range of wavelength defined by:

$$3.5d_j < \lambda < 7d_j \tag{17}$$

The jet diameter is slightly less than the internal capillary diameter. Equation 17 ensures that if the jet diameter is not accurately known, the apparatus may still be designed without risking the loss of the monodispersion in droplet diameters. The weight of the resulting droplets is equal to the weight of a cylinder having a diameter equal to the jet diameter and a height equal to the wavelength:

$$m = \frac{\pi}{6} d^3 = \frac{\pi}{4} d_j^2 \lambda \tag{18}$$

Combining Equations 16 and 18 leads to:

$$d = 1.89\ d_j \tag{19}$$

The drop size is thus directly correlated with the jet diameter, itself equal to or slightly less than the internal capillary diameter. The contraction of the jet at the exit of the capillary is due the pressure change, and the jet diameter will decrease slightly with the increase in jet speed.

The jet velocity must be lower than the terminal velocity of the droplets, as explained later. Except for this limitation, the jet velocity may be freely selected until the vibration frequency is adapted to maintain the wavelength in the range of values defined by Equation 17. Figure 6 shows that the terminal velocity and the minimal jet velocity curves cross at the droplet diameter equal to 380 μm. It would appear to be impossible to produce drops of a diameter smaller than 380 μm by jet breaking. However, Nir et al.[44] prepared beads as small as 30 μm with an apparatus similar to that illustrated in Figure 3. Hence, jet formation may not be necessary to initiate small droplet formation at the tip of a needle under vibration.

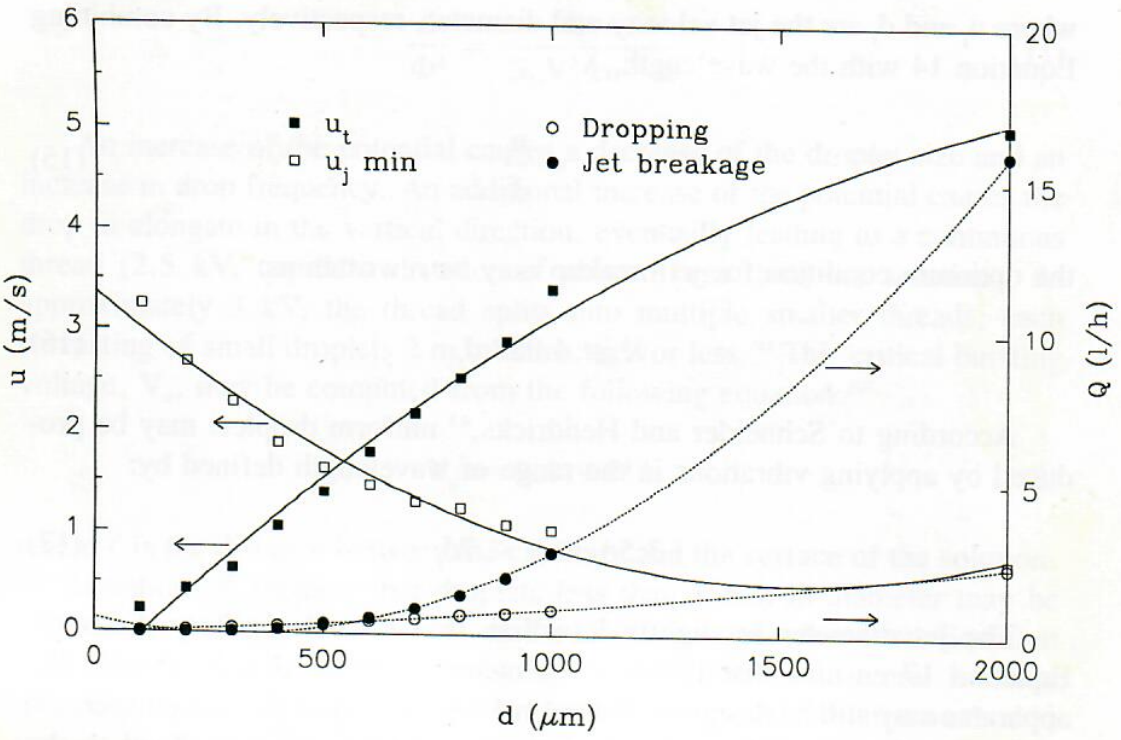

FIGURE 6. Influence of droplet diameter on volumetric flow rate.

E. EMULSIFICATION PROCESS

If beads are generally formed by the drop method, most of the membrane encapsulation procedures are based on emulsification of the core material in a nonmiscible phase. Due to scale-up problems with the drop method, several authors have recently considered emulsification as a potential technique for bead formation.[8,28,45]

In emulsification, droplets are not formed one by one, but rather in terms of millions by millions. The equations are thus built on a statistical basis, partially from mechanistic models and partially from empirical correlations. The fundamental analyses are principally based on the work of Kolmogorov[46] and Hinze.[47] These authors stated that the energy dissipated in a turbulent flow creates a viscous stress or a dynamic pressure which tends to break the drop. The surface tension force and the internal drop viscosity counteract these deformations.

The reactors used for emulsification are usually cylindrical vessels, mixed by means of an impeller. Baffles may be introduced in the vessel to improve the turbulence or mixing. The impeller may consist of a turbine with blades of various designs, a marine-style impeller, or a grid device. The emulsion may also be formed in other shear devices such as an open-tube static mixer (Figure 7). Because of the variety of designs, the nonengineer may be confused by the number of different correlations proposed to describe the dispersion in mixing devices. The biggest problem, in fact, is to define which design

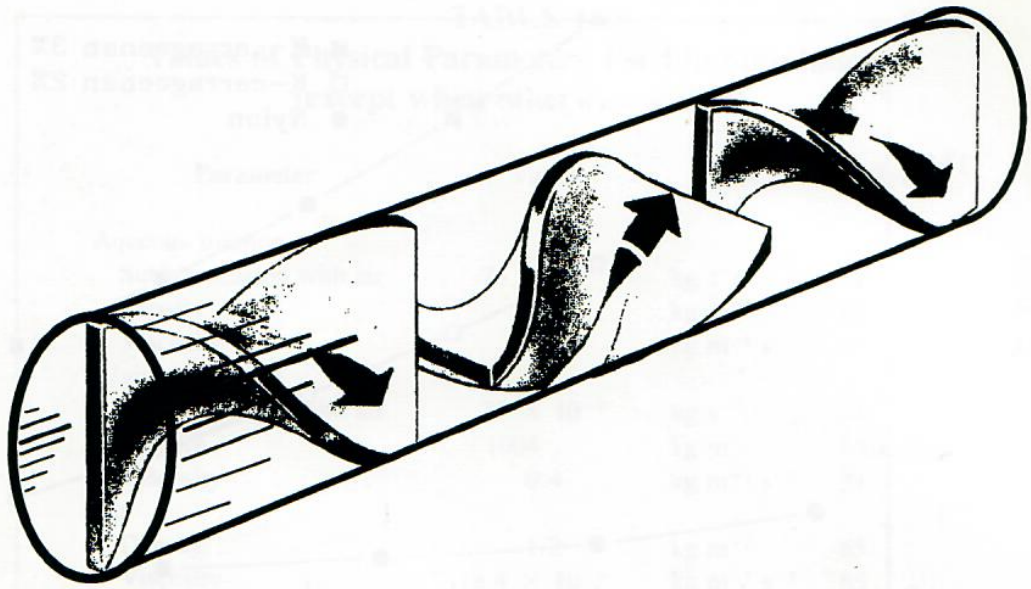

FIGURE 7. Design of a static mixer.

parameters must be involved in these relationships. Surprisingly, when this is done, a relatively simple and general equation may be written which derives from both mechanistic analyses and empirical correlations:[48]

$$\frac{d}{D} = k\, We^{-0.65}\, Re^{-0.2} \left(\frac{\mu d}{\mu}\right)^{0.5} \tag{20}$$

where D is the hydraulic diameter of the dispersion device (internal diameter for the static mixer, impeller diameter for the turbine reactor), k is a constant function of the design, and μ_d is the dispersed phase viscosity. We and Re are the Weber and Reynold's numbers defined by:

$$We = \frac{D\rho u^2}{\gamma} \tag{21}$$

and

$$Re = \frac{D\rho u}{\mu} \tag{22}$$

Equation 20 assumes that the parameters defining the final drop size are essentially the rotational speed of the impeller, the viscosity of both the continuous and dispersed phases, and the interfacial tension.

For a specific design, the choice of rotational speed permits the production of droplets ranging from a few micrometers[49] to a few hundred micrometers

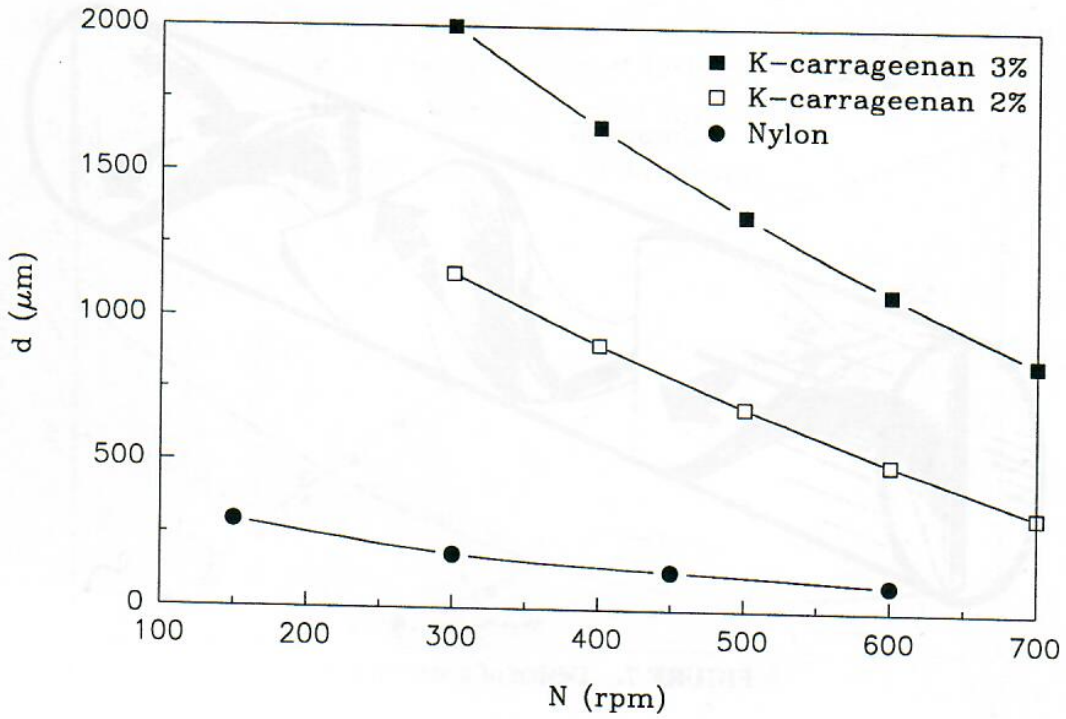

FIGURE 8. Correlation between droplet diameter and impeller rotational speed. (κ-Carrageenan data computed from Reference 28 and nylon data from Reference 29.)

(Figure 8).[29] The introduction of baffles associated with the operation of a turbine impeller helps to reduce the droplet size, but has a minimal impact when combined with other mixing devices.[9] Impellers which promote a homogeneous dispersion of the shear or mixing energy in the reactor, such as grid impellers, lead to lower droplet diameters with a narrower size distribution.[9,29,50] Increasing the surfactant concentration to lower the surface tension also reduces the microcapsule diameter.[29,50] The presence of different compounds in either the aqueous or the organic phase,[51] as well as variations in the pH of the aqueous phase,[52] act on the resultant droplet or microcapsule size, probably through a change in the dispersed phase viscosity and surface tension.

Audet and Lacroix[28] studied the effects of various formulation parameters on the diameters and size distribution of κ-carrageenan beads. The mean diameter of the bead preparations decreased with reduced gel concentrations and increased impeller rotational speeds (Figure 8). Beads were prepared in the range of 150 to 4000 μm.

In the case of alginate beads, gelification may be achieved by internal liberation of calcium by acidification.[8] The size distribution of the bead preparations is defined as much by the chemistry as the hydrodynamics.[9] Ideally, gelification should take place rapidly, but only after emulsion equilibrium is reached. This occurs when the rate of droplet coalescence equals the rate of break-up. Low levels of free calcium result in an initial gelification before

TABLE 1
Values of Physical Parameters Used in Simulations (except when otherwise stated)

Parameter	Value	Unit	Ref.
Aqueous solution			
Surface tension with air	73×10^{-3}	$kg\ s^{-2}$	21
Density	10^3	$kg\ m^{-3}$	65
Viscosity	10^{-3}	$kg\ m^{-1}\ s^{-1}$	65
Alginate solution			
Surface tension with air	73×10^{-3}	$kg\ s^{-2}$	34
Density	1004	$kg\ m^{-3}$	Measured
Viscosity	0.4	$kg\ m^{-1}\ s^{-1}$	34
Air			
Density	1.2	$kg\ m^{-3}$	65
Viscosity	18.4×10^{-6}	$kg\ m^{-1}\ s^{-1}$	65
Organic solvent (mixture of benzyne and tetrachloride)			
Surface tension with water	45×10^{-3}	$kg\ s^{-2}$	25
Density	10^3	$kg\ m^{-3}$	25
Viscosity	10^{-3}	$kg\ m^{-1}\ s^{-1}$	Assumed
Oil			
Surface tension with water	45×10^{-3}	$kg\ s^{-2}$	25
Density	960	$kg\ m^{-3}$	Measured
Viscosity	0.065	$kg\ m^{-1}\ s^{-1}$	Measured

this condition is attained. The use of calcium citrate as a calcium source and high guluronic alginate favors this primary gelification, leading to large-diameter beads (800 μm, Figure 9). Calcium carbonate and low guluronic alginate result in smaller-diameter beads (less than 300 μm). In intermediate conditions, the size distribution is multimodal (peaks at 250 and 800 μm, Figure 9). Using a grid impeller in place of a turbine or marine-style impeller and increasing the impeller rotational speed permits the formation of more homogeneous, smaller-diameter beads. The alginate viscosity and concentration as well as the surfactant concentration do not appear to influence the size distribution.

The actual data qualitatively represent the tendencies predicted by Equation 20; however, the fitting of data to this equation has not been successful. Equation 20 was designed for low discontinuous-phase concentrations and Newtonian fluids. Gel and preencapsulating solutions may behave in a non-ideal manner, resulting in deviations from the behavior predicted by Equation 20 for bead or microcapsule formation. The swelling or shrinkage of droplets during gelification and/or polymerization of the membrane constituents may lead to smaller or larger diameters than expected. Moreover, as in the case of alginate beads, other processes such as early gelification, which are not represented in the Equation 20 theory, may determine the final size.

The device most commonly used to form emulsions is the mechanically agitated vessel in which shear, energy dissipation, and dynamic pressure are

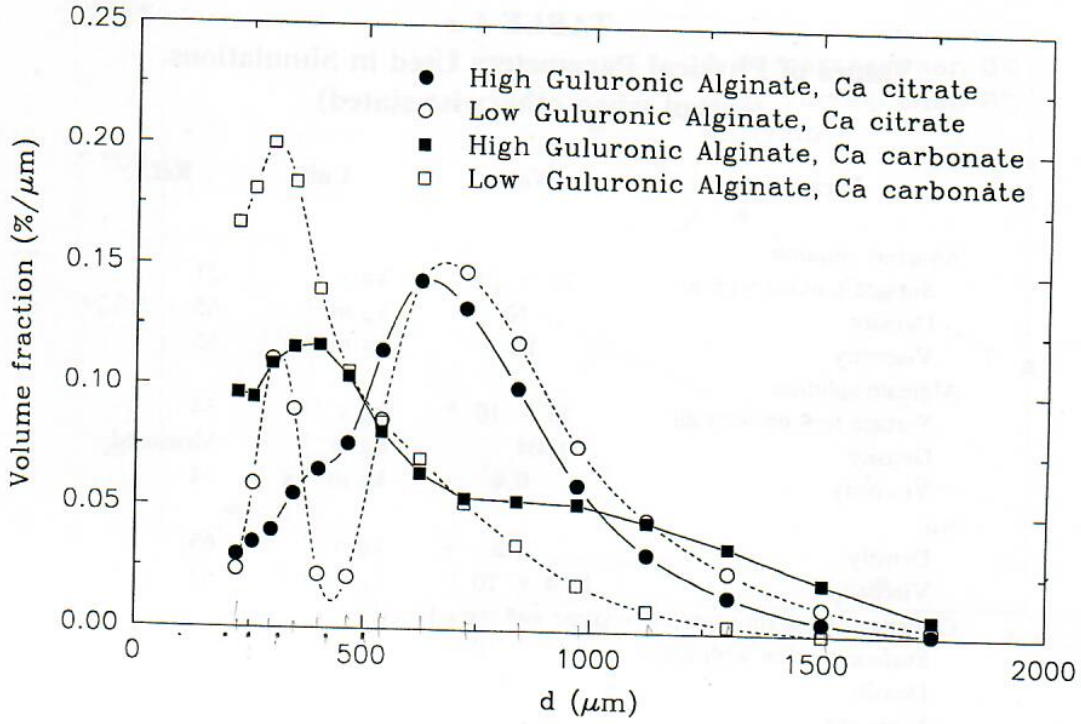

FIGURE 9. Impact of chemistry on alginate beads produced by emulsification techniques. Satellite peaks were removed.

not homogeneously distributed. In many vessels, dead volumes or stagnant zones may be present, particularly as the vessel volume increases or when mixing viscous fluids such as gels.[9] One alternative for minimizing these problems may be provided by static mixers. These devices consist of a series of stationary elements mounted lengthwise in a pipe (Figure 7). The elements form intersecting channels that split, rearrange, and recombine component streams into smaller and smaller layers. Mean diameters of the dispersed phase ranging from a few microns to 1 mm may be produced, and the droplet size defined by an equation similar to Equation 20 derived from mechanistic models.[53] Except for one industrial example, (Blachford, Montreal, Canada), static mixers have not been considered for bead or microcapsule production. This may be due to the fact that the minimal flow rate needed to operate static mixers is approximately 2 l/min, beyond that of the usual laboratory scale.

III. BEAD AND MICROCAPSULE SIZE DISPERSION

In the previous discussion, monodispersed preparations of carrier beads or capsules were assumed. However, fluctuations in the processes governing the phase dispersion step result in size dispersions in the final formulations. Monodispersed preparations are not strictly possible, and it is necessary to assess the extent of the size dispersion.

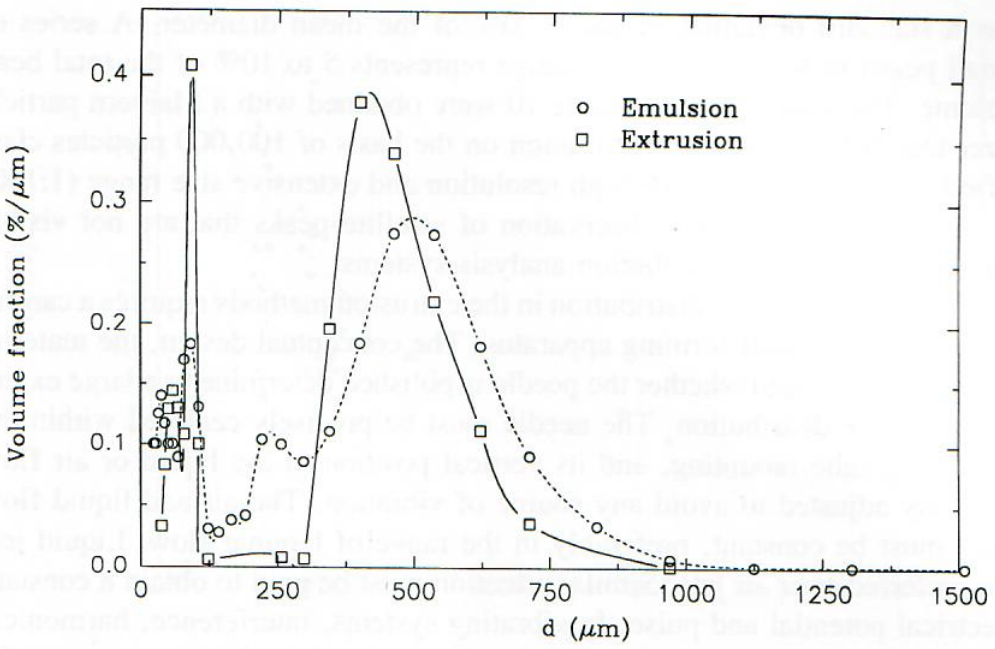

FIGURE 10. Comparison of the size distribution of alginate beads produced by emulsion and electric pulse extrusion methods.

Comparing size distributions extracted from different sources is often difficult. Instrumentation is costly and thus not in general use. Distributions obtained by sieving or microscopic measurement may be biased. Distribution data are generally presented on a numeric or volumetric basis, with the theoretical possibility of passing from one model to the other. In practice, establishing the distribution parameters is difficult. Monomodal distributions require at least three parameters of description (curve shape, mean, and dispersion values). For multimodal distributions, the number of parameters increases, and the same curve may thus be fitted successfully with several size distribution laws. In the following discussion, unless otherwise stated, the size distribution will be assumed to fit the normal law, and defined on the volumetric fraction basis, not on numerical frequency.

A. SIZE DISTRIBUTION OF DROPLETS PREPARED BY EXTRUSION

Any perturbations in air or liquid flow, electric field, or vibration during droplet generation will lead to variations in droplet diameter. Just prior to release from the needle, the droplets remain attached by a small liquid column. Turbulence or a vibration of even very small intensity is able to break this liquid cylinder. This secondary breakage leads to small droplet satellites. Finally, when the various droplets penetrate the collecting solution, they may break again, giving rise to even smaller droplets and/or satellites.

A typical size distribution of alginate beads prepared using an electric pulse extrusion apparatus is presented in Figure 10. The main symmetric peak

has a standard deviation of about 20% of the mean diameter. A series of small peaks in the low-diameter range represents 5 to 10% of the total bead volume. The data shown in Figure 10 were obtained with a Malvern particle sizer that defines the size distribution on the basis of 100,000 particles classified into 32 channels. The high resolution and extensive size range (1:100) of the instrument permits observation of satellite peaks that are not visible with most other size distribution analysis systems.

Narrowing the size distribution in the extrusion methods requires a careful design of the droplet-forming apparatus. The conceptual design, the material of construction, and whether the needle is polished determine to a large extent the final size distribution. The needle must be precisely centered within the concentric tube mounting, and its vertical position in the liquid or air flow carefully adjusted to avoid any source of vibration. The air and liquid flow rates must be constant, preferably in the range of laminar flow. Liquid jets are preferred over air jets. Similar attention must be paid to obtain a constant electrical potential and pulse. In vibrating systems, interference, harmonics, and reasonance are other causes of size dispersion. The distance between the needle tip and the collecting solution must be carefully adjusted.

The greater the force required to break the droplet, the higher will be the resultant size dispersion. Experience has shown that increasing the air-jet velocity increases both the size dispersion of the droplet and the spatial dispersion. The falling drops form a cone with an angle that increases with the air-jet velocity. The perturbations act more on small drops or jets, and the small jets are themselves more easily broken than the larger jets. This is observed by plotting the standard deviation as a function of droplet size; the size dispersion increases when the droplet size decreases (Figure 11).[34]

There are insufficient data to compare different extrusion methods. However, from the limited data available, it appears that the liquid-jet system leads to a smaller size dispersion, with standard deviations typically around 14%.[25] It may be noted that both this value and the results presented in Figure 11 probably underestimate the size dispersion, since they often do not account for the presence of satellite peaks.

B. SIZE DISTRIBUTION OF DROPLETS PREPARED BY EMULSIFICATION

Although it is generally believed that extrusion methods result in monodisperse preparations, this is not the case. Emulsification techniques, on the other hand, lead to even broader size distributions (Figure 10). Standard deviations may be as large as 70% in extreme cases.

Emulsification techniques may be classified into systems with or without coalescence. As in the case of the extrusion methods, satellite droplets are formed when a large droplet is broken (Figure 10). However, if coalescence is a dominant process, satellite droplets coalesce with larger drops, in which

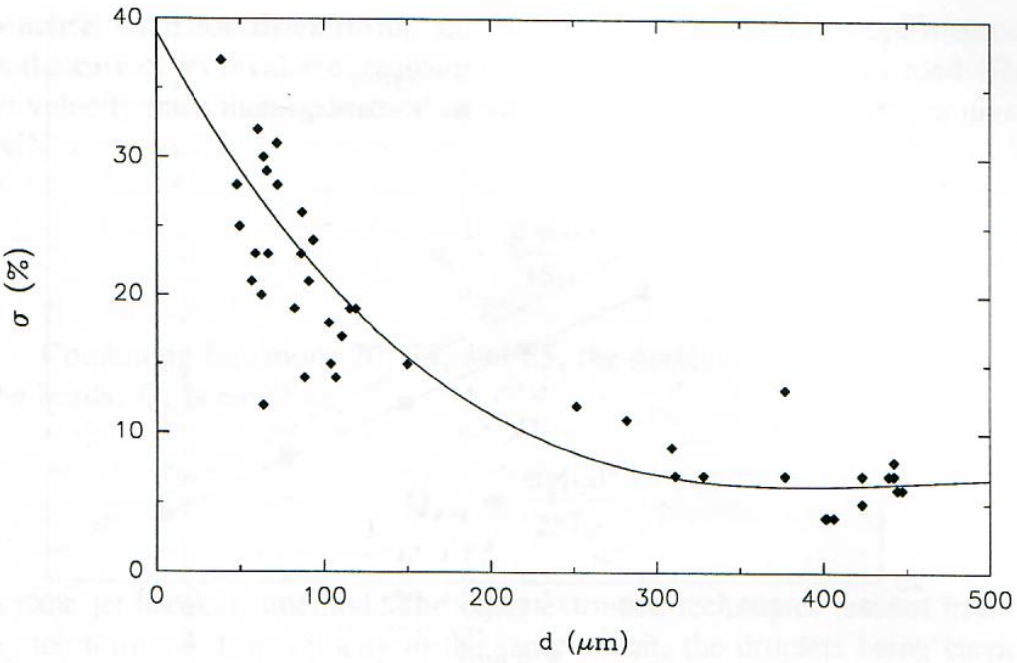

FIGURE 11. Relationship between relative standard deviation and diameter of alginate beads produced by coaxial air-jet extrusion. (Computed from data of Reference 34.)

case the satellite peaks may account for less than 1% of the particle volume,[29] leading to a narrower global size dispersion.

The main peak of the distributions is generally best represented by a normal or log-normal law.[28,29] The standard deviation generally ranges between 30 and 70% of the mean, and decreases with the impeller speed, and thus the mean droplet diameter in turbine mixers (Figure 12).[28,29] This trend is the reverse of that obtained with extrusion methods, in which the size distribution increases as the droplet diameter decreases. Narrower distributions are obtained by using impellers that distribute the mixing energy uniformly, such as the grid frame,[9,29] when increasing the surfactant concentration and reducing both the viscosity and density ratios of the dispersed vs. continuous phase.[29]

With alginate beads, even broader size distributions are obtained (Figure 9). The presence of several peaks results in a high global standard deviation value. However, attention to the gelification conditions of the system and the judicious design of the impeller and reactor may result in the standard deviation being reduced to a value approaching 30% of the mean.[9]

One of the main reasons for the broad diameter distribution is the non-homogeneity of the shear in the turbine reactor.[54] The static mixer may offer better control of the diameter of carrier particles formed by an emulsification method. Each droplet is subject to a more homogeneous shear, resulting in a more uniform breakage. Several authors[48,55] reported standard deviation values as low as 17 to 23%, values similar to that observed when using the extrusion methods.

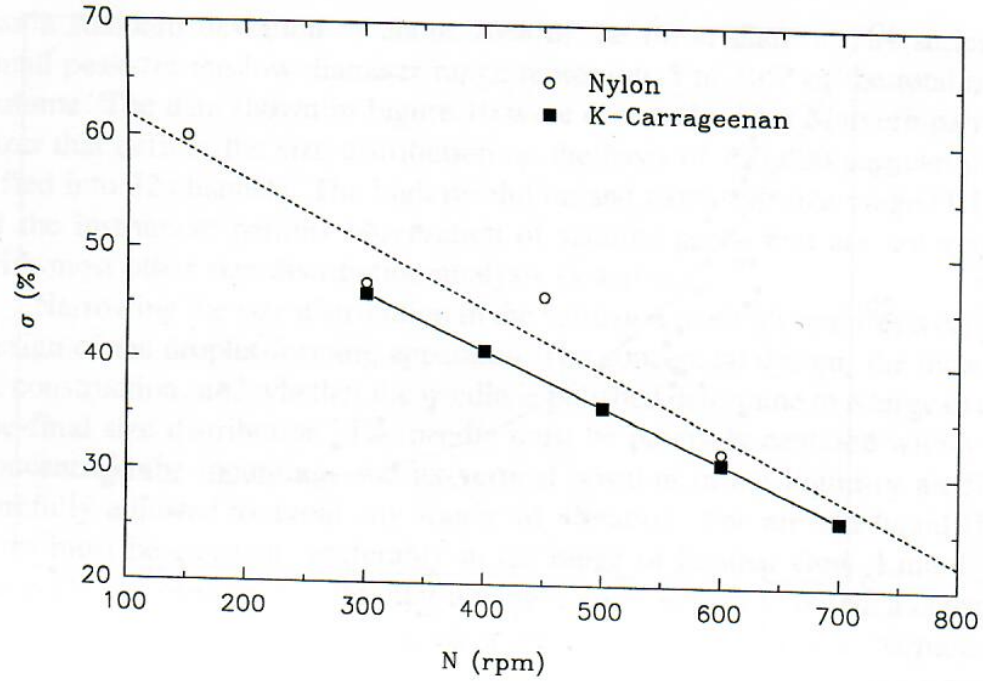

FIGURE 12. Standard deviation of κ-carrageenan beads and nylon microcapsules as a function of impeller rotational speed. (Computed from data of References 28 and 29.)

IV. SCALE-UP OF DISPERSION PROCESSES

A. EXTRUSION METHODS

In the extrusion method, the volumetric droplet flow, Q, is equal to:

$$Q = \frac{\pi}{4} d_j^2 u_j \tag{23}$$

where d_j and u_j are the diameter and velocity, respectively, of the jet or, by extrapolation, of the fluid inside the needle. Except for the jet breakage method, the velocity of the fluid in the needle must be lower than the minimum velocity for jet formation, $u_{j,min}$, which was found to be dependent on the surface tension, s, the liquid density, r, and the jet diameter, d_j:[56]

$$u_{j,min} \geq 2\sqrt{\frac{\sigma}{\rho d_j}} \tag{24}$$

By combining Equation 23 and 24 (replacing d_j by d, Equation 19), one obtains:

$$Q_{max} = 0.19\pi\sqrt{\frac{\sigma}{\rho}d^3} \tag{25}$$

which is valid for all extrusion techniques except the jet breakage method. In the case of jet breakage, collisions between droplets must be avoided. The jet velocity must then be lower than the terminal velocity of the droplet given by:[57]

$$u_t = \frac{g\,\rho_d d^2}{18\mu} \tag{26}$$

Combining Equations 20, 23, and 25, the maximum volumetric flow of the beads, Q, is equal to:

$$Q_{max} = \frac{\pi g \rho_d d^4}{257\mu} \tag{27}$$

for the jet breakage method. The other extrusion techniques are not limited by the terminal drop velocity to the same extent, the droplets being carried by the liquid or gas flow at a velocity up to ten times higher or by an electric field considerably larger than the gravitational field.

The maximum flow rate for various extrusion methods is plotted in Figure 6. Hulst et al.[27] reported that uniform 2- to 3-mm alginate beads were formed at a liquid flow rate of up to 24 l/h. However, with smaller-diameter beads and microcapsules, the maximum flow rate when preparing 100-μm-diameter beads is limited for all extrusion methods to approximately a few milliliters per hour. This is considerably less than the production rate needed for many food or environmental applications, where cubic-meter volumes of beads may be required.

Researchers generally assume that the low production rate of droplets formed by extrusion methods may be resolved by the use of multiple needles or extrusion ports. The limitation of production rate is critical for small droplets (Figure 6), since the diameter is sensitive to the operating conditions and perturbations, as shown by the large size distribution (Figure 11). Variation in the diameter leads to dispersion of the falling drop velocity, increasing the risk of collisions between droplets in the same stream. Moreover, the drop streams diverge, defining a cone under the tip of the extruding needle. The cone angle increases as the drop diameter decreases. The risk of collisions between droplets coming from different needles is thus increased for small drops.

For multiple-needle operation, the breakage force must be applied carefully and uniformly to each needle, increasing the operational difficulties as the number of ports increases. Dabora[58] proposed reducing the risk of droplet collision by applying opposite charges to alternate needles and reversing the charge on the needles after the formation of each droplet. This complex system has been proved partially successful with a 21-hole spray.

The scale-up of extrusion methods, especially for small-droplet formation, remains a difficult problem.

B. EMULSIFICATION METHOD

Scale-up of emulsification techniques for bead or microcapsule production is much less of a problem than with extrusion methods. Chang and Poznansky,[59] when initially preparing microcapsules in a beaker with a magnetic stirrer, operated with microcapsule volumes of approximately 1 ml, illustrating the limited scale of operation of early workers in the field. In contrast, the use of a static mixer permits flow rates of 2 l/min, up to cubic meters per minute, and has been applied industrially in microencapsulation (Blachford, Montreal, Canada). Batches of microcapsules or beads have been prepared in turbine reactors with volumes of hundreds of milliliters in less than 15 min.[28] The principal limitation in the scale-up of an emulsification process for biological cells is probably the increase of the shear stress as the size of the reactor increases.

V. SHEAR DURING ENCAPSULATION

One of the principal objectives in cell encapsulation is to protect cells from shear damage. It follows that the cells must be immobilized under nondisruptive conditions. Researchers generally neglect the possibility of cell damage during extrusion and assume a high risk with the emulsification methods even though little evidence is available to confirm or to refute these assumptions.

Cell disruption during immobilization may be due to several factors. Shear is applied to the cell suspension during extrusion from a needle during droplet formation. This shear may be caused by mixing forces within a droplet, and pressure variations and disruptive forces during jet or droplet breakup. Only some of these effects may be quantified. The droplet pressure in the needle bore may be computed by the Hagen-Poiseuille equation.[60,61] The average shear rate in the needle bore or in the turbine reactor may be computed from the fluid velocity distribution.[31] Maximum shear rate in the turbine reactor may be estimated from relationships available in the literature.[62] For Newtonian fluids, shear stress is equal to the product of shear rate and viscosity. Table 2 summarizes disruptive forces in various dispersion systems, computed from the relationships outlined above. Some caution must be exercised when using these results. For example, the static mixer was simulated by an open tube with a half-diameter during shear estimation, and the transversal shear was not taken into consideration. Also, the scale of the different processes is different.

Most forces acting on the cells are proportional to the suspension viscosity. Shear stress, for example, is the product of the shear rate and viscosity. The

TABLE 2
Disruptive Forces in Dispersion Systems

Parameter	Extrusion tube	Turbine reactor	Static mixer
Flow (ml min^{-1})	1.5		670
Reactor volume (ml)		1000	
Tube length (cm)	20		25.4
Tube diameter (mm)	7.62		0.7
Reactor diameter (mm)		108	
Turbine diameter (mm)		54	
Turbine speed (s^{-1}/rpm)		5/300	
Fluid (m s^{-1})	0.065		0.304
Tip speed (m s^{-1})		0.339	
Shear rate[a] (s^{-1})	371	12.8/47[a]	160
Shear stress (kg m^{-1} s^{-2})	148	0.816	10.4
Shear period (s)	0.39	900	0.07
Pressure drop (atm)	4.3		0.011

Note: Forces computed assuming alginate bead diameter of 300 μm, dispersed oil (see Table 1 for other physical parameter values).

[a] Average/maximum.

formation of high-viscosity gel beads (0.4 kg m^{-1} s^{-1}) may initiate greater damage than the formation of microcapsules from a low-viscosity solution (10^{-3} kg m^{-1} s^{-1}). Disruptive effects on the cells are dependent on the period of application and probably proportional to the product of the time period and the shear stress. Pressure disruptive forces are more related to the ratio of the pressure vs. the time period. The shear effect in the turbine may then be larger than expected from the shear stress itself due to the long application time of the disruptive forces. In contrast, the scale-up with a static mixer is achieved by increasing the pipe diameter, keeping the fluid velocity, and thus the shear rate, quasiconstant. Shear effects on living cells may be considered by extrapolating from studies on microcapsule breakage[17] in a mixing environment. Shear damage was related to the fourth power of the spherical diameter. Large cells may rupture in systems that are compatible with smaller biological cells such as bacteria or yeast. Shear sensitivity is also determined by the membrane properties of the cell. A cell wall-defective mutant of green algae was sensitive to a stress 20 times less than that exhibited by wild-type strains (Table 3).[63] Similarly, it is recognized that animal and insect cells are more fragile than plant cells.

Bronnemeier and Märkl[63] compared a free-jet system with a turbine reactor in terms of impact on the production rate, release of cell contents, and aggregate disruption. They defined a critical stress capacity when the effect of the disruptive forces was initially observed and correlated this parameter to the energy dissipated per unit of volume (Table 3). The critical stress capacity,

TABLE 3
Critical Stress Capacity of Cell Cultures[63]

Culture and characteristics	Free jet		Turbine	
	ΔP (atm)	E (W/l)	Ω (rpm)	E (W/l)
Chlorella vulgaris				
Green alga, 5–6 μm	>100		>2700	
Anacystis nidulan				
Blue-green alga, 0.2–2 μm	≈100		>2700	
Chlamydomonas reinhardi				
(Wild-type strain) green alga 4–12 μm	17	5.5	2400	41
Cell wall-defect mutant strain	1	0.11	300	0.3
Spirula platensis				
Prokaryotic 15-μm filament aggregates	3	0.4	900	3.9

expressed in energy dissipated, was seven times lower with the free jet than with the mixing jet.

At similar levels of energy dissipation, cultures appear to be more sensitive to disruptive forces during extrusion than during mixing,[63] possibly due to the fact that the energy in the free jet is dissipated in a smaller volume than in a mixing reactor. Moreover, the gel surrounding the cell may reduce the mixing effects while increasing the disruptive force in the extrusion.

It is difficult to draw conclusions concerning disruptive forces based on the available data. Further studies should be undertaken to define the most suitable reactor design for cell encapsulation.

VI. CELL DISTRIBUTION BETWEEN CARRIER BEADS

When entrapping lactic acid bacteria (up to 10^{10} cells per ml) within large-diameter beads (2.5 mm), the distribution of cells between the beads may be assumed to be uniform (10^9 cells per bead). This is no longer the case with smaller-diameter microcapsules, as the cell size is more similar to the microcapsule size. Nir et al.[44] found that the cell distribution, after encapsulation in 10- to 40-μm-diameter beads, could be defined by the Poisson distribution:

$$P(m,n) = \frac{m^n e^{-m}}{n!} \tag{28}$$

where P(m,n) is the percent of beads containing n cells when the average number of cells is m. Figure 13 shows the percent of capsules containing one or more cells as a function of the average number of cells per bead. The number of cells must be at least three or five times larger than the number of carrier beads to ensure that less than 5 or 1% of the beads, respectively,

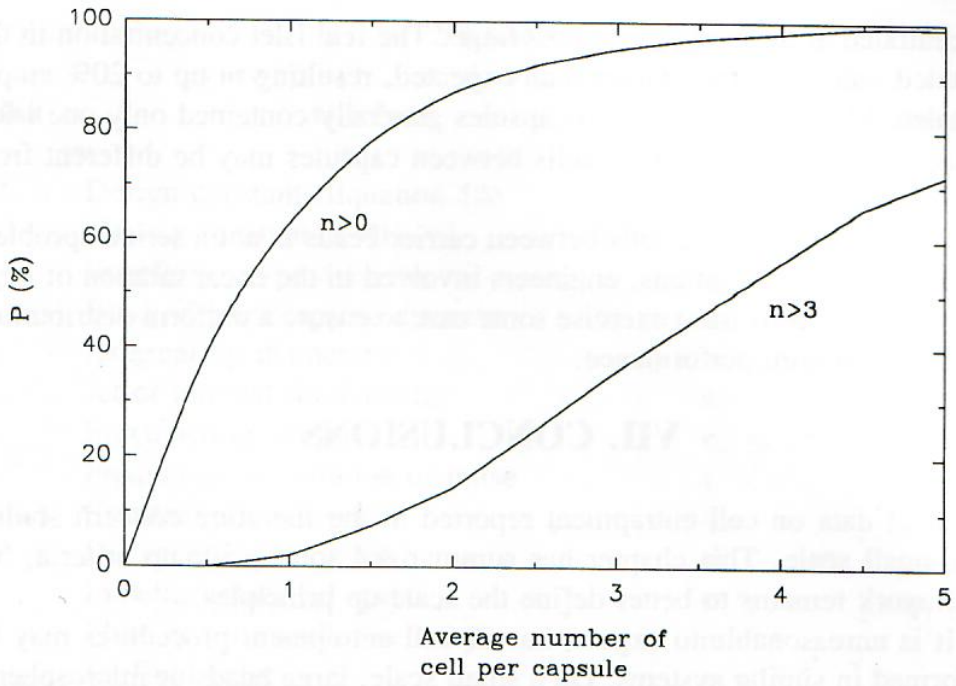

FIGURE 13. Distribution of cells between capsules.

will not contain a cell. For small bacterial cells with concentrations to 10^{10} cells per ml, the size of the microcapsules may be reduced to 10 μm without encountering inhomogeneity. This is no longer the case if the cells form colonies or aggregates, or for larger-diameter cells.

When encapsulating islets of Langerhans for treatment of diabetes, it is desirable to ensure that most microcapsules contain a single islet cell. The diameter of the islets range from 100 to 200 μm; thus, to be injectable by syringe into the peritoneal cavity, the capsules must contain no more than two or three islets. This results in 15% of the microcapsules being void of cells (Figure 13). This also assumes that the initial concentration of islets is sufficiently large. For microcapsules of 400-μm diameter, the initial concentration of islets would need to be 30,000 islets per ml, a concentration which is difficult to attain.

Several authors reported that a significant number of carrier beads were empty of cells following the encapsulation of islets in small alginate or Eudragit beads (700 μm). The following calculation may illustrate the problem. The islet concentration is typically 1000 islets per ml. If 6000 beads of 700-μm diameter are produced from 1 ml of gel, theoretically only 16% of the beads will contain an islet.

Sun et al.[64] reported that 20% of microcapsules were void of cells. Equation 27 was demonstrated for small-diameter cells. The behavior of suspensions of large cells may be different. In Nir's study,[44] no settling of the cells would be expected. In lab-scale experiments, the islets settled and were

concentrated at the bottom of the syringe. The real islet concentration in the extruded volume is then larger than expected, resulting in up to 20% empty capsules. Moreover, most microcapsules generally contained only one islet. Hence the distribution law of cells between capsules may be different from one system to another.

If the distribution of cells between carrier beads is not a serious problem for high cell concentrations, engineers involved in the encapsulation of large or aggregative cells must exercise some care to ensure a uniform distribution, and thus optimum performance.

VII. CONCLUSIONS

Most data on cell entrapment reported in the literature concern studies on a small scale. This chapter has summarized some scale-up criteria, but much work remains to better define the scale-up principles.

It is unreasonable to expect that all cell entrapment procedures may be performed in similar systems. On a small scale, large beads or microspheres with a narrow size distribution may be achieved using extrusion methods. Beads larger than 300 μm may be formulated at higher production rates by jet breakage. Extrusion with liquid coaxial jets appears to provide a smaller dispersion, but very little data exist on this particular system. For very-large-scale efforts with small microcapsule diameters, emulsification techniques should be used. Static mixers may help to obtain a narrower size distribution with minimal cell damage, but they have not been tested for cell encapsulation.

This chapter may serve as a needed starting point for future studies dedicated to scale-up problems in cell encapsulation.

SYMBOLS

Symbol	Gradeur	S.I. unit	Usual unit(s)
a	Design constant (Equation 10)	—	
g	Gravity constant (9.81)	$m\ s^{-2}$	
D	Impeller or pipe diameter	m	
d	Bead or microcapsule diameter	m	μm
d_e	External tip diameter	m	mm or μm
d_j	Jet or internal tip diameter	m	μm
F	Force acting on drops	$kg\ m\ s^{-2}$	N
f	Frequency of vibration or pulse	s^{-1}	
k	Constant (Equation 20)	—	
l	Distance (Equation 10)	m	cm
N	Impeller rotational speed	s^{-1}	rpm
u	Fluid or tip impeller velocity	$m\ s^{-1}$	
u_j	Jet fluid velocity	$m\ s^{-1}$	
m	Mass of the drop	kg	
Q	Fluid flow rate	$m^3\ s^{-1}$	$l\ h^{-1}$
Q_{max}	Maximum fluid flow rate	$m^3\ s^{-1}$	$l\ h^{-1}$
Re	Reynold's number (Equation 22)	—	
V	Electric potential	V	
V_c	Critical bursting voltage	V	
We	Weber's number (Equation 21)	—	
α	Angle (Figure 6)	—	
γ	Interfacial or surface tension		
Φ	Ratio of the real and ideal drop diameters		
μ	Continuous phase viscosity	$kg\ m^{-1}\ s^{-1}$	
μ_d	Dispersed phase viscosity	$kg\ m^{-1}\ s^{-1}$	cp
ρ	Continuous phase density	$kg\ m^{-3}$	
ρ_d	Dispersed phase density	$kg\ m^{-3}$	

REFERENCES

1. **Cheetham, P. S. J., Blunt, K. W., and Bucke, C.,** Physical studies on cell immobilization using calcium alginate gels, *Biotechnol. Bioeng.*, 21, 2155, 1979.
2. **Hackel, U., Klein, J., Megnet, R., and Wagner, F. W.,** Immobilisation of microbial cells in polymeric matrices, *Eur. J. Appl. Microbiol.*, 1, 291, 1975.
3. **Siess, M. H. and Divies, C.,** Behaviour of *Saccharomyces cerevisiae* cells entrapped in a polyacrylamide gel and performing alcoholic fermentation, *Eur. J. Appl. Microbiol. Biotechnol.*, 12, 10, 1981.
4. **Umemura, I., Takamatsu, S., S., Sato, T., Tosa, T., and Chibata, I.,** Improvement of production of L-aspartic acid using immobilized microbial cells, *Appl. Microbiol. Biotechnol.*, 20, 291, 1984.
5. **Cheetham, P. S. J., Garett, C., and Clark, J.,** Isomaltulose production using immobilized cells, *Biotechnol. Bioeng.*, 27, 471, 1985.
6. **Yokoyama, K., Saka, F., Kai, T., and Soeda, E.-I.,** Encapsulation of cells in agarose beads for use in the construction of human DNA libraries as yeast artificial chromosomes (YAC), *Jpn. J. Hum. Genet.*, 35, 131, 1990.
7. **Audet, P., Paquin, C., and Lacroix, C.,** Immobilized growing lactic acid bacteria with κ-carrageenan-locust bean gum gel, *Appl. Microbiol. Biotechnol.*, 29, 11, 1988.
8. **Lencki, R. W. J., Neufeld, R. J., and Spinney, T.,** Method of Producing Microspheres, U.S. Patent 4,822,534, 1989.
9. **Poncelet, D., Beaulieu, C., Hallé, J. P., Fournier, A., and Neufeld, R. J.,** Large scale production of alginate beads using emulsions, *Appl. Microbiol. Biotechnol.*, in press.
10. **Lim, F. and Sun, A. M.,** Microencapsulated islets as bioartificial endocrine pancreas, *Science*, 210, 908, 1980.
11. **Birnbaum, S., Pendleton, R., Larsson, P. O., and Mosbach, K.,** Covalent stabilization of alginate gel for the entrapment of living whole cells, *Biotechnol. Lett.*, 3(8), 393, 1981.
12. **Hwang, C., Rha, C. K., and Sinskey, A. J.,** Encapsulation with chitosan: transmembrane diffusion of proteins in capsules, in *Chitin in Nature and Technology*, 1986, 389.
13. **Rha, C. and Rodriguez-Sanchez, D.,** Process for Encapsulation and Encapsulated Active Material System, European Patent 0 152 898 A2, 1985; Massachusetts Institute of Technology, U.S. Patent Appl. 85101490.2, 1985.
14. **Larroche, C. and Gros, J.-B.,** Batch and continuous 2-heptanone production by Ca-alginate/Eudragit RL entrapped spores of *Penicillium roquefortii*, *Biotechnol. Bioeng.*, 34, 30, 1989.
15. **Larisch, B. C., Poncelet, D., Neufeld, R. J., and Champagne, C. P.,** Microencapsulation of *Lactococcus lactis* subsp. *cremoris* for application in the dairy industry, *J. Dairy Sci.*, submitted.
16. **Poncelet, D., Poncelet De Smet, B., and Neufeld, R. J.,** Nylon membrane formation in biocatalyst microencapsulation: physicochemical modelling, *J. Membr. Sci.*, 50, 249, 1990.
17. **Poncelet, D. and Neufeld, R. J.,** Shear breakage of nylon membrane microcapsules in a turbine reactor, *Biotechnol. Bioeng.*, 33, 95, 1989.
18. **Warren, G. S. and Fallon, R.,** Reversible, lectin-mediated immobilization of plant protoplasts on agarose beads, *Planta*, 161, 201, 1984.
19. **Neufeld, R. J., Peleg, Y., Rokem, J. S., Pines, P., and Goldberg, I.,** L-Malic acid formation by immobilized Saccharomyces cerevisiae amplified for fumarase, *Enzyme Microb. Technol.*, 13, 991, 1991.
20. **Chang, T. M. S., MacIntosh, F. C., and Mason, S. G.,** Semipermeable aqueous microcapsules. I. Preparation and properties, *Can. J. Physiol. Pharmacol.*, 44, 115, 1966.

21. **Harkins, W. D. and Brown, F. E.,** The determination of surface tension and the weight of falling drops, *J. Am. Chem. Soc.*, 41, 499, 1919.
22. **Poncelet, D., Poncelet De Smet, B., and Neufeld, R. J.,** Mass transfer in nylon membrane bound microcapsules, paper presented at 38th Canadian Chemical Engineering Conf., October 2 to 5, 1988.
23. **Okahata, Y., Hachiya, S., and Nakamura, G. I.,** Permeability of large polyamide microcapsule coated with synthetic bilayer membrane, *Chem. Lett.*, 1719, 1982.
24. **Miyawaki, O., Nakamura, K., and Yano, T.,** Permeability and molecular sieving characteristics of nylon microcapsule membrane, *Agric. Biol. Chem.*, 44(12), 2865, 1980.
25. **Charwat, A. F.,** Generator of droplet tracers for holographic flow visualization in water tunnels, *Rev. Sci. Instrum.*, 48(8), 1034, 1977.
26. **Hommel, M., Sun, A. M., and Goosen, M. F. A.,** Droplet Generation, Canadian Patent, 1,241,598, 1988.
27. **Hulst, A. C., Tramper, J., Van't Riet, K., and Westerbeek, J. M. M.,** A new technique for the production of immobilized biocatalyst in large quantities, *Biotechnol. Bioeng.*, 27, 870, 1984.
28. **Audet, P. and Lacroix, C.,** Two-phase dispersion process for the production of biopolymer gel beads: effect of various parameters on bead size and their distribution, *Proc. Biochem.*, December, 217, 1989.
29. **Poncelet De Smet, B., Poncelet, D., and Neufeld, R. J.,** Preparation of hemolysate-filled hexamethylene sebacamide microcapsules with controlled diameter, *Can. J. Chem. Eng.*, 68, 443, 1990.
30. **Lane, W. R.,** A microburette for producing small liquid drops of known size, *Rev. Sci. Instrum.*, 24, 98, 1947.
31. **Bird, R. B.,** *Transport Phenomena,* John Wiley & Sons, New York, 1960.
32. **Foscolo, P. U., Gibilaro, L. G., and Waldram, S. P.,** A unified model for particulate expansion of fluidised beds and flow in fixed porous media, *Chem. Eng. Sci.*, 38(8), 1251, 1983.
33. **Miyawaki, O., Nakamura, K., and Yano, T.,** Microencapsulation of urease by interfacial polymerization with liquid-air nozzle method, *Agric. Biol. Chem.*, 43(5), 1133, 1979.
34. **Su, H., Bajpai, R., and Preckshot, W.,** Characterization of alginate beads formed by a two fluid annular atomizer, *Appl. Biochem. Biotechnol.*, 20/21, 561, 1989.
35. **Nukiyama, S. and Tanazawa, Y.,** *Kikai Gakkei Ronbunshu,* 5, 136, 1939.
36. **Dupuy, B., Gin, H., Bacquey, C., and Ducassou, D.,** Technique de microencapsulation de cellules dans de l'agarose, *Innov. Tech. Biol. Med.*, 7(5), 628, 1986.
37. **Gin, H., Baquey, C., Ducassou, D., and Dupuy, B.,** Maintained activity of living cells microencapsulated in a polymerized medium, *C. R. Soc. Biol.*, 182(1), 79, 1988.
38. **Dupuy, B., Gin, H., Baquey, C., and Ducassou, D.,** *In situ* polymerization of a microencapsulating medium round living cells, *J. Biomed. Mater. Res.*, 22(11), 1061, 1988.
39. **Nawab, M. A. and Mason, S. G.,** The preparation of uniform emulsion by electrical dispersion, *J. Colloid Sci.*, 13(2), 179, 1957.
40. **Arakawa, M. and Kondo, T.,** Preparation and properties of poly(*N,N*-L-lysinediylterephthaloyl) microcapsules containing hemolysate in the nanometer range, *Can. J. Physiol. Pharmacol.*, 58, 183, 1980.
41. **Savart, F.,** *Ann. Chim.*, 53, 337, 1833.
42. **Rayleigh, J. W. S.,** On the instability of jet, *Proc. London Math. Soc.*, 10, 4, 1878.
43. **Schneider, J. M. and Hendricks, C. D.,** Source of uniform sized liquid droplets, *Rev. Instrum.*, 35, 1349, 1964.
44. **Nir, R., Lamed, R., Gueta, L., and Sahar, E.,** Single-cell entrapment and microcolony development within uniform microspheres amenable to flow cytometry, *Appl. Environ. Microbiol.*, 56(9), 2870, 1990.

45. **Chibata, I., Tosa, T., and Sato, T.,** Immobilized cells in preparation of fine chemicals, *Adv. Biotechnol. Proc.*, 1, 203, 1983.
46. **Kolmogorov, A. N.,** The breakup of droplets in a turbulent stream, *Dok. Akad. Nauk.*, 66, 825, 1949.
47. **Hinze, J. O.,** Fundamentals of the hydrodynamic mechanism of splitting in dispersion processes, *AIChE J.*, 1, 289, 1955.
48. **Haas, P. A.,** Turbulent dispersion of aqueous drops in organic liquids, *AIChE J.*, 33(6), 987, 1987.
49. **Shiba, M., Tomioka, S., Koishi, M., and Kondo, T.,** Studies on microcapsules. V. Preparation of polyamide microcapsules containing aqueous protein solution, *Chem. Pharm. Bull.*, 18(4), 803, 1970.
50. **Poncelet De Smet, B., Poncelet, D., and Neufeld, R. J.,** Control of mean diameter and size distribution during formulation of microcapsules with cellulose nitrate membranes, *Enzyme Microb. Technol.*, 11, 29, 1989.
51. **Shigeri, Y., Koishi, M., Kondo, T., Shiba, M., and Tomioka, S.,** Studies on microcapsules. VI. Effect on variations in polymerization conditions on microcapsule size, *Can. J. Chem.*, 48, 2047, 1970.
52. **Poncelet, D., Alexakis, T., and Neufeld, R. J.,** Microencapsulation within cross-linked polyethyleneimine membranes, *J. Microencap.*, in press.
53. **Middleman, S.,** Drop size distributions produced by turbulent pipe flow of immicible fluids through a static mixer, *Ind. Eng. Chem. Process. Des. Dev.*, 13(1), 78, 1974.
54. **Tanaka, M.,** Local droplet diameter variation in a stirrer tank, *Can. J. Chem. Eng.*, 63, 723, 1985.
55. **Streiff, F.,** In-line dispersion and mass transfer using static mixing equipment, *Sulzer Technol. Rev.*, 3, 108, 1977.
56. **Lindblad, N. R. and Schneider, J. M.,** Production of uniform-sized liquid droplets, *J. Sci. Instrum.*, 42, 635, 1965.
57. **Stoke, G. C.,** On the effect of the internal friction of the fluids on the motion pendulum, *Trans. Cambridge Philos. Soc.*, 9, 8, 1851.
58. **Dabora, E. K.,** Production of monodisperse sprays, *Rev. Sci. Instrum.*, 38(4), 502, 1967.
59. **Chang, T. M. S. and Poznansky, M. J.,** Semipermeable aqueous microcapsules (artificial cells). V. Permeability characteristics, *J. Biomed. Mater. Res.*, 2, 187, 1968.
60. **Poiseuille, J.,** *Compte Rendus*, 11, 961, 1041, 1840.
61. **Hagen, G.,** *Ann. Phys. Chem.*, 46, 423, 1839.
62. **Wichterle, K., Kadlec, M., Zak, L., and Mitschka, P.,** Shear rates on turbine impeller blades, *Chem. Eng. Commun.*, 26, 25, 1984.
63. **Bronnemeier, R. and Märkl, H.,** Hydrodynamic stress capacity of microorganisms, *Biotechnol. Bioeng.*, 24, 533, 1982.
64. **Sun, A. M., O'Shea, G., van Roy, H., and Goosen, M.,** Microencapsulation d'îlots de Langerhans et pancréas artificiel, *J. Annuel. Diabetol. Hotel*, 161, 1982.
65. **Weast, R. C. and Astle, M. J.,** *CRC Handbook of Chemistry and Physics*, CRC Press, Boca Raton, FL, 1982.